HHS Public Access

Author manuscript

Biometrics. Author manuscript; available in PMC 2018 April 28.

Published in final edited form as:

Biometrics. 2017 June ; 73(2): 367–377. doi:10.1111/biom.12613.

A Subgroup Cluster-Based Bayesian Adaptive Design for Precision Medicine

Wentian Guo[1], **Yuan Ji**[2,3,*], and **Daniel V. T. Catenacci**[4,5]

[1]Department of Biostatistics, School of Public Health, Fudan University, Shanghai, China

[2]Program of Computational Genomics and Medicine, Northshore University HealthSystem

[3]Department of Public Health Sciences, The University of Chicago, Chicago, U.S.A

[4]Department of Medicine, Section of Hematology and Oncology

[5]University of Chicago Medical Center, Chicago, U.S.A

Summary

In precision medicine, a patient is treated with targeted therapies that are predicted to be effective based on the patient's baseline characteristics such as biomarker profiles. Oftentimes, patient subgroups are unknown and must be learned through inference using observed data. We present SCUBA, a Subgroup ClUster-based Bayesian Adaptive design aiming to fulfill two simultaneous goals in a clinical trial, 1) to treatments enrich the allocation of each subgroup of patients to their precision and desirable treatments and 2) to report multiple subgroup-treatment pairs (STPs). Using random partitions and semiparametric Bayesian models, SCUBA provides coherent and probabilistic assessment of potential patient subgroups and their associated targeted therapies. Each STP can then be used for future confirmatory studies for regulatory approval. Through extensive simulation studies, we present an application of SCUBA to an innovative clinical trial in gastroesphogeal cancer.

Keywords

Adaptive design; Bayesian nonparametrics; Dirichlet process; Enrichment designs; Personalized therapy; Reversible jump MCMC

1. Introduction

1.1. Background

Patient heterogeneity is now widely known for many diseases, such as cancer (Catenacci, 2015). Inter-tumor heterogeneity refers to the differences in the basic biology, development, and response to a treatment across different tumors. Different from one-size-fits-all

* koaeraser@gmail.com.

Supplementary Materials

Web Appendices, Tables, and Figures referenced in Sections 1.2, 2.4, and 3.2 are available with this article at the *Biometrics* website on Wiley Online Library. A C++ binary executive file, which can be used to conduct SCUBA analysis, and an example of R script for plotting the reported STPs are also given on the website along with data from a selected trial of Scenario 1.

approaches such as the traditional chemo or radiation therapies, precision medicine treats subgroups of patients with targeted therapies based on the heterogeneity in their molecular profiles and baseline characteristics. Some molecular targeted medications have been successfully developed for subgroups of patients. For example, trastuzumab induces better response in breast cancer patients with overexpressed HER2 than those who do not. The pair of (HER2+ breast cancer, trastuzumab) is a simple example of precision medicine as the use of trastuzumab relies on a single biomarker, HER2. Currently, there is increasing effort looking for more pairs of targeted drugs and corresponding biomarkers (e.g., NCI MATCH Trial, Mullard, 2015).

Only dozens of subgroup treatment pairs (STPs) like (HER2+ breast cancer, Trastuzumab) have been discovered and marketed for cancer care. Many more effective STPs are yet to be identified, partly due to lack of statistical methods for subgroup discovery and analysis. Early work in Simon and Maitournam (2004) and Maitournam and Simon (2005) discussed in theory the efficiency and sample size of targeted trials compared to randomized clinical trials (RCT). Sargent et al. (2005) presented a biomarker-by-treatment interaction design and biomarker-based-strategy design, where the former was an extension of RCT with biomarkers as stratification, and the latter used the biomarker as the identifier of whether to use a particular treatment. Freidlin et al. (2010) compared different biomarker-RCT schemes. All of these methods assume that a fixed number of prespecified subgroups is available, and test if treatments would exhibit varying therapeutic effects on different subgroups. There is no notion of learning new subgroups as all subgroups are predetermined. This could be problematic if predefined subgroups are not predictive of outcomes or treatment selection. An example is the BATTLE trial (Kim et al., 2011). BATTLE is a pioneering study to test treatment and biomarker interactions using a fixed-subgroup design. The design prespecified five subgroups based on 11 selected biomarkers, and randomized patients within each subgroup to different treatments using response-adaptive randomization. Kim et al. (2011) concluded that the biomarker groups used in BATTLE were less predictive than were individual biomarkers, making them clinically less appealing.

In light of the lesson learned from previous studies, the field has shifted to methods that allow new subgroups to be discovered during and after the clinical trial. Sivaganesan et al. (2011) and Laud et al. (2013) transformed the subgroup identification problem to a model selection problem among different partition models. Ruberg et al. (2010), Foster et al. (2011), and Lipkovich et al. (2011) conducted subgroup analysis by looking for regions in covariate space that have significantly different response rates compared to the average response rate. Zhao et al. (2013) presented a scoring function of multiple baseline covariates to estimate subject-specific treatment differences, based on a working response-covariate model. Berger et al. (2014) proposed a Bayesian model selection approach based on random trees for subgroup identification, in which continuous response variable and binary covariates are considered. Shen and He (2015) proposed a confirmatory statistical test for the existence of subgroups by using a structured logistic-normal mixture model. Green and Kern (2012) used Bayesian additive regression trees (BART) (Chipman et al., 2010) to identify treatment effect heterogeneity among different subgroups. Lastly, Xu et al. (2014) proposed a subgroup enrichment design, SUBA, aiming to allocate patients to subgroup-

specific treatments. Their approach uses a tree-type of random clustering model that splits the biomarker space using the median of observed values for each biomarker. We will show later that SCUBA extends the SUBA model with more realistic boundaries to split the biomarker space, while retaining the enrichment feature in SUBA.

1.2. Motivating Trial

We consider a novel clinical trial in gastroesophageal adenocarcinoma (GEC). GEC is the third most common malignancy and the second most common cause of death world-wide. It is a molecularly heterogeneous disease as tumor heterogeneity between patients is believed to be a driving factor for treatment selection (Catenacci, 2015). The biomarker trial of GEC is called PANGEA (funded by National Institute of Health, NCT02213289), which is currently based on a design that addresses tumor heterogeneity by assigning treatments according to predefined predictive molecular "oncogenic driver" categories, namely, genes *HER2, MET, FGFR2, EGFR/HER3*, and *KRAS/PI3K*. Most of the molecular measurements are continuous protein expressions. The PANGEA protocol includes comprehensive molecular profiling of the tumor at diagnosis on the primary tumor and at a metastatic disease site (liver, lung, or peritoneum) at enrollment. All patients will be assigned to one of five specific treatments based on the metastatic tumor molecular profile. See Web Appendix A for a description.

Since the existing design of PANGEA only specifies the allocation of therapies to patients based on predetermined subgroups as the first-line treatment, clinicians face challenges in patient allocation in the case of disease progression after first-line treatment. We propose to enhance the design of PANGEA trial and aim for an improved patient allocation strategy after first-line targeted therapy. In the new design, patients whose first-line treatments have failed will be allocated based on the protein expression of several biomarkers measured for the recurrent lesions, and adaptively allocated to the optimal treatment predicted by the new design. We are in the process of preparing a new protocol for a new trial, which we tentatively call PANGEA 2.

1.3. Overview of SCUBA

In PANGEA 2, the biomarkers are protein expressions and the outcome is a binary response variable after treatment of cancer. Therefore in SCUBA, we consider a design for trials with continuous biomarkers and binary outcomes. A brief discussion of extending SCUBA to accommodate discrete covariates and continuous or survival outcomes is given at the end.

We use lines/planes/hyperplanes to partition the continuous biomarker space and define subgroups. As a result, patient subgroups are defined as polygons bounded by hyperplanes in the biomarker space. This is a linear approximation to the true subgroups, which may have nonlinear and irregular-shaped boundaries. The linear approximation, however, allows for efficient model construction and posterior inference. We show that the approximation works well in simulations. Additionally, SCUBA allows a different subset partition for each treatment. The number of linear boundaries in the biomarker space is assumed random, which allows data-driven inference. We develop a Markov chain Monte Carlo (MCMC) scheme to realize the posterior inference.

In SCUBA, a subset in the form of a polygon is associated with a response rate for a treatment. In other words, patients whose biomarker values fall into the subset are assumed to have the same response rate to the treatment. An important feature of SCUBA is that it borrows strength across subsets by assuming a Dirichlet process prior (Ferguson, 1973; Neal, 2000; Hjort et al., 2010) for the response rates across subsets. Therefore, subsets that are geographically distant in the biomarker space can still share the same response rate. This feature allows meaningful subgroup reporting at the end of the trial. For example, SCUBA can report winning subgroup-treatment pairs (STPs), each of which serves as a candidate of future confirmatory studies. This is in the heart of precision medicine. In summary, a clinical trial based on SCUBA will achieve two goals: 1) to enrich the allocation of patients to their precise treatments during the course of the trial and 2) to report STPs at the end of the trial for future confirmatory studies.

The remainder of the article is organized as follows. Section 2 describes the probability model and posterior inference. We present the SCUBA design in Section 3 and its application to the PANGEA 2 trial in Section 4. Section 5 concludes with a brief discussion.

2. Probability Model

2.1. Linear Boundary

Suppose under consideration is a total of B biomarkers and T candidate treatments, indexed by $b = 1, \cdots, B$ and $t = 1, \cdots, T$, respectively. Let x_b, $b = 1, \cdots, B$ denote a continuous measurement of biomarker b, such as protein expression. For mathematical convenience, we assume that $x_b \in [-1, 1]$ has been standardized. In the upcoming discussion, we assume that the subgroup boundaries are treatment specific. That is, the biomarker space is partitioned differently for different treatments. This would require the partition-related parameters having the treatment index t for mathematical symbols. For simplicity, we suppress the index t in this subsection and will put it back afterwards. models.

We introduce hyperplanes as linear boundaries in the biomarker space $\Omega = [-1, 1]^B$ to define patient subgroups. A linear boundary in the B-dimensional biomarker space Ω can be written as a linear equation, $\sum_{b=1}^{B} \beta_b x_b = c$, where β_b's and c are real values. This general format does not give a unique solution as multiple β's and c's can give the same boundary. To get the unique solution, we impose a constraint, $\sum_{b=1}^{B} \beta_b^2 = 1$, on β_b's. When $B = 2$, one natural way to impose this constraint is re-parametrizing the linear equation to $\sqrt{1 - r^2} x_1 + r x_2 = c$, where $r \in (-1, 1]$. Similarly, when $B = 3$, one natural way to impose this constraint is re-parametrizing the linear equation to $\sqrt{1 - r_1^2} x_1 + r_1 \sqrt{1 - r_2^2} x_2 + r_1 r_2 x_3 = c$, where $r_1, r_2 \in (-1, 1]$. By deduction, a linear boundary s in the B–dimensional biomarker space Ω when $B > 1$ can be written as a standardized linear equation, given by

$$\sum_{b=1}^{B-1} \left(\prod_{s'=1}^{b-1} r_{s,s'} \right) \sqrt{1 - r_{s,b}^2} \cdot x_b + \prod_{s'=1}^{B-1} r_{s,s'} \cdot x_B = c_s, \quad s = 1, \ldots, S, \quad (1)$$

where $r_{s,b} \in (-1, 1]$ and S is the number of boundaries. When $B = 1$, the boundary can be written as $x_1 = c_s$, $s = 1,\ldots,S$ without slope parameters. We assume hereinafter $B > 1$, and remedy to the case when $B = 1$ can be easily made by ignoring the slope r. Since $x_b \in [-1, 1]$ and $r_{s,b} \in (-1, 1]$, it follows that $|c_s| \leq \sqrt{B}$, $\forall s$. It can be easily shown that for $r_{s,b} \in (-1, 1]$ and $c_s \in [-\sqrt{B}, \sqrt{B}]$ there is a 1-to-1 mapping between a linear hyperplane in Ω and $(r_{s,1}, \ldots, r_{s,B-1}, c_s)$. This facilitates the prior construction for $r_{s,b}$ and c_s later. According to (1), the tuple $r_s = (r_{s,1}, \ldots, r_{s,B-1})$ decides the "direction" of the s^{th} boundary and c_s affects the "intercept" of the boundary.

For each direction, we allow up to two parallel linear boundaries to give more flexibility in modeling the biomarker-response surfaces. For example, sometimes response to a treatment is associated with complex interaction of multiple biomarkers, resulting in a nonlinear biomarker-response surface for both biomarkers (Ala et al., 2013).

In other words, we allow $0 \leq M_s \leq 2$ boundaries with the same direction $\boldsymbol{r}_s$, $s = 1, \ldots, \boldsymbol{B}$. This is realized by having M_s number of intercepts $c_{s,a}$, where subscript a's index the intercepts with the same direction. Altogether, we allow up to $2 \times B$ hyperplanes as subgroup boundaries. Therefore, changing c_s to $c_{s,a}$ we rewrite (1) as

$$\sum_{b=1}^{B-1} \Big(\prod_{s'=1}^{b-1} r_{s,s'} \Big) \sqrt{1 - r_{s,b}^2} \cdot x_b + \prod_{s'=1}^{B-1} r_{s,s'} \cdot x_B = c_{s,a}, \quad a = 1, \ldots, M_s. \qquad (2)$$

Figure 1 gives an example of boundaries in the case of two biomarkers. There are two directions in Figure 1, with one direction having two lines (dashed) and the other direction having only one line (dotted). Without loss of generality, assume the intercept parameter $c_{s,a}$ is increasing with respect to the index a, that is, $c_{s,a_1} > c_{s,a_2}$ when $a_1 > a_2$. This construction avoids label switching in the posterior inference (McLachlan and Peel, 2004).

2.2. Likelihood Function

Hereinafter, we add subscript t to all parameters to allow treatment-specific partitions. For treatment t, define $\boldsymbol{r}_t = \{r_{t,s}, s = 1, \ldots, \boldsymbol{B}\}$ where $\boldsymbol{r}_{t,s} = \{r_{t,s,b}, b = 1, \ldots, B - 1\}$ is the s^{th} direction, $\boldsymbol{c}_t = \{\boldsymbol{c}_{t,s}, s = 1,\ldots, B\}$ where

$$\boldsymbol{c}_{t,s} = \begin{cases} \varnothing & \text{if } M_{t,s} = 0, \\ \{c_{t,s,1}\} & \text{if } M_{t,s} = 1, \\ \{c_{t,s,1}, c_{t,s,2}\} & \text{if } M_{t,s} = 2, \end{cases}$$

is the s^{th} intercept set for direction $\boldsymbol{r}_{t,s}$, and $\boldsymbol{M}_t = \{M_{t,s}, s = 1,\ldots,B\}$ with $M_{t,s}$ denoting the number of boundaries for direction $\boldsymbol{r}_{t,s}$.

Parameters $(\boldsymbol{r}_t, \boldsymbol{c}_t, \boldsymbol{M}_t)$ and their priors induce a random partition $\prod_t$ for treatment t on the biomarker space Ω. We write the partition $\prod_t = \{A_{t,1}, \cdots, A_{t,I_t}\}$, where $A_{t,i}$ is the i^{th} partition

set for treatment t, $i = 1, \ldots, I_t$, and I_t is the random number of partition sets for treatment t. A saturated partition has $M_{t,s} = 2$ boundaries for all directions s $\in\{1, \cdots, B\}$, and every pair of boundaries for one direction intersects the pair of boundaries for another direction. In such a case, there are $I_t = 3^B$ partition sets for treatment t. In general, $I_t \leq \prod_{s=1}^{B}(M_{t,s}+1)$.

We consider y_j, the binary outcome for patient j. Let $\boldsymbol{X}_j = (X_{j,1}, \ldots, X_{j,B})$ be the observed biomarker profile and t_j the treatment assignment for patient j, $j = 1, \cdots, n$, respectively. Define $\theta_{t,i} = Pr(y_j = 1 \mid t_j = t, \boldsymbol{X}_j \in A_{t,i})$, the response probability for patients in partition set $A_{t,i}$ for treatment t. The observed data consist of $(y_j, \boldsymbol{X}_j, t_j)$ for all the patients that have been enrolled in the trial. Define $\boldsymbol{y} = \{y_1, \cdots, y_n\}$, $\boldsymbol{X} = \{\boldsymbol{X_1}, \cdots, \boldsymbol{X}_n\}$, $\boldsymbol{t} = \{t_1, \cdots, t_n\}$, $\boldsymbol{\theta} = (\boldsymbol{\theta}_1, \ldots, \boldsymbol{\theta}_t)$ and $\boldsymbol{\theta}_t = (\theta_{t,1}, \ldots, \theta_{t,I_t})$, $\boldsymbol{c} = (\boldsymbol{c}_1, \ldots, \boldsymbol{c_T})$, $\boldsymbol{M} = (\boldsymbol{M}_1, \ldots, \boldsymbol{M}_T)$, $\boldsymbol{r} = (\boldsymbol{r}_1, \ldots, \boldsymbol{r}_T)$, and $\prod = (\prod_1, \ldots, \prod_T)$. The likelihood function is given by

$$\boldsymbol{L}(\boldsymbol{y} \mid \boldsymbol{\theta}, \boldsymbol{\Pi}) = \prod_j \left\{ \sum_{i=1}^{I_{t_j}} \theta_{t_j,i} \times \mathbf{1}(\boldsymbol{X}_j \in A_{t_j,i}) \right\}^{y_j} \times \left\{ 1 - \sum_{i=1}^{I_{t_j}} \theta_{t_j,i} \times \mathbf{1}(\boldsymbol{X}_j \in A_{t_j,i}) \right\}^{1-y_j}, \quad (3)$$

where only one indicator $\mathbf{1}(\boldsymbol{X}_j \in A_{t_j,i})$ equals 1 for patient j across all partition sets i, and the remaining indicators are 0 for the patient.

2.3. Prior Models

The joint Bayesian hierarchical model can be written as

$$\boldsymbol{L}(\boldsymbol{y} \mid \boldsymbol{\theta}, \boldsymbol{\Pi}) p(\boldsymbol{\theta} \mid \boldsymbol{\Pi}) \prod_{t=1}^{T} p(\boldsymbol{\Pi}_t \mid \boldsymbol{c}_t, \boldsymbol{r}_t, \boldsymbol{M}_t) p(\boldsymbol{c}_t, \boldsymbol{r}_t, \boldsymbol{M}_t). \quad (4)$$

In (4), $p(\prod_t \mid \boldsymbol{c}_t, \boldsymbol{r}_t, \boldsymbol{M}_t) \equiv 1$ since $(\boldsymbol{c}_t, \boldsymbol{r}_t, \boldsymbol{M}_t)$ deterministically decides the partition $\prod_t$. We only need to specify the prior $p(\boldsymbol{c}_t, \boldsymbol{M}_t, \boldsymbol{r}_t)$.

Assuming the intercept $\boldsymbol{c}_t$ and the slope $\boldsymbol{r}_t$ are independent given $\boldsymbol{M}_t$, we have $p(\boldsymbol{c_t}, \boldsymbol{r_t}, \boldsymbol{M}_t) = p(\boldsymbol{c}_t \mid \boldsymbol{M}_t) p(\boldsymbol{r}_t \mid \boldsymbol{M}_t) p(\boldsymbol{M_t})$. We allow $\boldsymbol{M}_{t,s}$ to be 0, 1 or 2, and assume a discrete uniform prior with $Pr(M_{t,s} = 0) = Pr(M_{t,s} = 1) = Pr(M_{t,s} = 2) = 1/3$. We construct priors for $\boldsymbol{r}_{t,s}$ and $\boldsymbol{c}_{t,s}$ conditional on $M_{t,s}$. The dimension of $\boldsymbol{c}_{t,s}$ is $M_{t,s}$. When $M_{t,s} = 0$, let $\boldsymbol{c}_{t,s} = \varnothing$. Since $|\boldsymbol{c}_{t,s,a}| \leq \sqrt{B}$, we assume uniform priors as below:

$$c_{t,s,1} \mid M_{t,s} > 0 \sim unif(-\sqrt{B}, \sqrt{B}),$$

$$c_{t,s,2} \mid c_{t,s,1}, M_{t,s} = 2 \sim unif(c_{t,s,1}, \sqrt{B}).$$

Note that the prior model forces $c_{t,s,2} > c_{t,s,1}$ to avoid label switching. Similarly, we take $unif[-1, 1]$ for priors of direction parameters r's.

To complete the prior construction in the model, we propose a Dirichlet process (DP) prior as $p(\boldsymbol{\theta} \mid \prod)$:

$$\theta_{t,i} \mid \boldsymbol{\Pi} \overset{iid}{\sim} G, \quad t = 1, \ldots, T, \quad i = 1, \ldots, I_t$$

$$G \sim DP(\alpha_0, Beta(a_0, b_0)).$$

We set $\alpha_0 = a_0 = b_0 = 1$. The base measure is then $Beta(1, 1)$, a uniform distribution. The natural clustering characteristic of DP induces possible clusters for the response rates $\{\theta_{t,i}\}$ across treatments and partition sets. This allows borrowing strength using data from all the patients.

2.4. Posterior Inference

Based on the joint model (4), posterior samples for the parameters are obtained using MCMC simulations. Sampling $M_{t,s}$ among values in 0, 1, or 2 might change the dimension of $\boldsymbol{c}_{t,s}$, $\boldsymbol{r}_{t,s}$, and $\boldsymbol{\theta}_t$. Hence, we make use of reversible jumps (Green, 1995; Richardson and Green, 1997). We make a random choice between changing the value of $M_{t,s}$ to an adjacent status or keeping $M_{t,s}$ at the current value.

Detailed description of the MCMC moves can be found in Web Appendix B. Using the posterior samples for all the parameters, we infer the posterior predictive probability described in Section 3.1 and the estimated subgroup-treatment pairs in Section 3.2.

3. The SCUBA Design

3.1. Patient Allocation

For a new patient enrolled in the trial, SCUBA calculates the posterior predictive probability of response under each treatment to guide the treatment assignment. Suppose the trial has accumulated data for n patients, including their biomarker profiles, treatment allocations, and responses, denoted by $\boldsymbol{X}^n$, $\boldsymbol{t}^n$, and $\boldsymbol{y}^n$, respectively. Based on the MCMC samples $\{(\boldsymbol{\theta}^{(k)}, \boldsymbol{c}^{(k)}, \boldsymbol{M}^{(k)}, \boldsymbol{r}^{(k)}), k = 1, \cdots, K\}$, the posterior predictive probability of response under treatment t for the $(n+1)^{th}$ patient with biomarker profile $\boldsymbol{X}_{n+1}$ is given by

$$\begin{aligned} q_{n+1}(t) &= Pr(y_{n+1} = 1 \mid \boldsymbol{X}_{n+1}, t_{n+1} = t, \boldsymbol{y}^n, \boldsymbol{X}^n, \boldsymbol{t}^n) \\ &= \sum_{\boldsymbol{M}} \int Pr(y_{n+1} = 1 \mid \boldsymbol{X}_{n+1}, t_{n+1} = t, \boldsymbol{\theta}, \boldsymbol{c}, \boldsymbol{M}, \boldsymbol{r}) p \times (\boldsymbol{\theta}, \boldsymbol{c}, \boldsymbol{M}, \boldsymbol{r} \mid \boldsymbol{y}^n, \boldsymbol{X}^n, \boldsymbol{t}^n) d\boldsymbol{r} d\boldsymbol{c} d\boldsymbol{\theta} \\ &\approx \frac{1}{K} \sum_{k=1}^{K} Pr(y_{n+1} = 1 \mid \boldsymbol{X}_{n+1}, t_{n+1} = t, \boldsymbol{\theta}^{(k)}, \boldsymbol{c}^{(k)}, \boldsymbol{M}^{(k)}, \boldsymbol{r}^{(k)}). \end{aligned}$$

Depending on the purpose of the trial, SCUBA allows adaptive randomization based on $q_{n+1}(t)$ or optimal treatment allocation by choosing the treatment $\hat{t}$ with the highest posterior predictive probability, that is,

$$\hat{t} = \arg\max_{t} q_{n+1}(t). \quad (5)$$

Adaptive randomization allocates patient $(n+1)$ to treatment t with a probability proportional to $q_{n+1}(t)$. The randomization mitigates potential selection bias and steers patient allocation toward the more precise and desirable treatment. On the other hand, optimal treatment allocation is typically used when an equal-randomization run-in phase is employed and the goal is to maximize the benefits for future patients by providing the optimal precise treatments for them. In Section 3.3, we present a version of SCUBA that uses a run-in phase and optimal treatment allocation.

3.2. Report Subgroup-Treatment Pair (STP)

One unique feature of SCUBA is that it can report multiple STPs in multi-arm clinical trials. We will show later in simulation studies this approach works quite well in finding the true STPs with low false discovery rates.

Reporting STPs hinges on the discovery of regions in the biomarker space Ω in which one treatment outperforms all the others. We define an equally spaced grid of H values $\{x_{b,1},\ldots, x_{b,H}\}$ for the biomarker b where each $x_{b,h} \in [-1, 1]$. Taking the Cartesian product of the grids across all B biomarkers, we obtain a B–dimensional grid $\tilde{x}$ of size H^B points. In the MCMC samples, the k^{th} iteration generates a set of boundaries on Ω for each treatment t, denoted by $(\boldsymbol{M}_t^{(k)}, \boldsymbol{c}_t^{(k)}, \boldsymbol{r}_t^{(k)})$. These boundaries subsequently define partition sets $\prod_t^{(k)} = \left\{A_{t,1}^{(k)}, \ldots, A_{t,I_t^{(k)}}^{(k)}\right\}$. For each grid point $\tilde{x}_h, h = 1, \ldots, H^B$, we can find the partition set $At, i(k)$ so that $\tilde{x}_h \in A_{t,i}^{(k)}$. Knowing now the partition set $At, i(k)$ we record the vector of response rates as $\boldsymbol{\theta}_h^{(k)} = (\hat{\theta}_{1,h}^{(k)}, \ldots, \hat{\theta}_{T,h}^{(k)})$ from the same MCMC iteration, which consists of response rates under all different treatments. The collection over all the MCMC iterations, $\left\{\boldsymbol{\theta}_h^{(k)}, k = 1, \ldots, K\right\}$ can be used to report the best treatment for the h^{th} grid point. For example, given a desired confidence $(1 - \alpha)$, $\alpha \in (0, 1)$, we select the "winning" treatment $\hat{t}h$ for the h^{th} grid point if

$$\hat{Pr}\left(\theta_{\hat{t}_h,h} > \max_{t \neq \hat{t}_h} \theta_{t,h}\right) = \frac{1}{K}\sum_k \mathbf{1}\left(\hat{\theta}_{\hat{t}_h,h}^{(k)} > \max_{t \neq \hat{t}_h} \hat{\theta}_{t,h}^{(k)}\right) > 1 - \alpha. \quad (6)$$

If $\hat{Pr}(\theta_{\tilde{t},h} > \max_{t \neq \tilde{t}} \theta_{t,h}) \leq 1 - \alpha, \forall \tilde{t} \in \left\{1, \cdots, T\right\}$, we do not report any winning treatment $\hat{t}h$ for the grid point $\tilde{x}h$ and set $\hat{t}_h = \varnothing$. Then over all the grid points, the collection

$\{(\hat{t}_h, \tilde{x}_h), h = 1, \ldots, H\}$ provides a map of STPs on the biomarker space, allowing blank space to indicate undecided regions. We show this in the simulation study next.

Alternatively, Web Appendix C provides a conditional posterior inference based on MCMC samples, which generates estimated partitions of the biomarker space as well as recommended STPs. The conditional inference is an approximation of the joint inference approach above. However, the conditional inference uses linear boundaries in closed forms for STPs, which can be easily interpreted. Depending on the need in practice, either STP reporting can be used.

3.3. Trial Design

The proposed SCUBA design consists of two phases (Box 1 below), a run-in phase during which patients are equally randomized to treatments, and an adaptive phase during which patients are allocated to t^ defined in Section 3.1. After the initial run-in phase, we update the posterior distributions once a new patient's response is obtained. The trial continues until the maximum sample size N is reached.

4. Results

4.1. Simulation Setup

We carry out simulation studies based on the PANGEA 2 trial to evaluate the performance of the SCUBA design. We plan to evaluate multiple treatments as the second-line therapies for patients with recurrent tumors or failing the first-line treatment. Expression from protein biomarkers will be considered to define patient subgroups. A binary response is defined as whether or not a patient has complete response to the treatment. We consider seven scenarios, scenarios 0–6, in the simulation studies. A total of 1000 trials is simulated under each scenario. We fix the maximum sample size of each simulated trial at $N = 400$, and the number of patients in the run-in period at $n = 300$. Therefore, in each simulated trial 300 patients will be equally randomized and 100 patients adaptively allocated. When $n \gg (N - n)$, most patients will be equally randomized and it is reasonable to use adaptive allocation without randomization for the remaining $(N - n)$ patients. Otherwise, we recommend to adaptively randomize the $(N - n)$ patients with a probability proportional to $q_j(\hat{t})$ for patient j. All the biomarker values are generated independently from a uniform (−1, 1) distribution. For reversible jumps, we set transition probability in MCMC as $P_{01} = P_{00} = P_{21} = P_{22} = 0.5$, $P_{10} = P_{11} = P_{12} = 1/3$.

For comparison, we apply SUBA and BART for each simulated trial, with the same number of patients for run-in and adaptation. The hyperprior parameters for SUBA are set to be the same as those in Xu et al. (2014). For BART, we use the "BayesTree" R package (https://cran.rproject.org/web/packages/BayesTree/index.html) and its default settings, with 500 posterior draws kept after 100 burn-in draws. The BART model is fitted with treatment and biomarkers as covariates whenever a new patient's data are collected, and the adaptive allocation of the future patient is guided by posterior predictive probabilities of the BART model. As SUBA and BART do not provide a formal way to report the STPs, we only

compare the performance of allocating patients to their corresponding targeted therapies under three methods.

Scenario 0 is a null case in which response rates under $T = 2$ treatments are not related to any biomarkers. Regardless of the biomarker values, the response rate for each treatment is 0.4. This scenario monitors the false positive reporting of the designs.

In scenario 1, there are $B = 2$ biomarkers x_{j1} and x_{j2} and $T = 3$ treatments. The response rate of each treatment is assumed to be associated with biomarker values in the following way. Let $\tilde{\theta}_{tj}$ be the true response rate for patient j under treatment t. We assume

$$\tilde{\theta}_{1j} = \Phi_{0,1.5}(x_{j1} + 1.5x_{j2}), \quad \tilde{\theta}_{2j} = \Phi_{0,1.5}(x_{j1}),$$

$$\tilde{\theta}_{3j} = \Phi_{0,1.5}(x_{j1} - 1.5x_{j2}),$$

where $\Phi_{\mu,\sigma}(x)$ is the cumulative distribution function (CDF) of a Gaussian distribution evaluated at point x, with mean μ and standard deviation σ. Figure 2 displays the monotone response surfaces versus biomarkers 1 and 2 under each treatment. Either treatment 1 or 3 is the best treatment with the highest response rate, depending on if $x_2 > 0$. Specifically, treatment 1 is the best treatment when $x_2 > 0$ and treatment 3 is the best treatment when $x_2 < 0$. Therefore, $x_2 = 0$ is the true subgroup boundary. Note that this boundary coincides with the median of x_2. Since the SUBA design uses empirical medians of observed biomarker values as boundaries, we expect SUBA to perform well in this scenario.

In scenario 2, $T = 3$ treatments are considered and $B = 3$ biomarkers are related to their response rates. The true response rates are given by

$$\tilde{\theta}_{1j} = \Phi_{0,1.5}(x_{j1} + 1.5x_{j2} - 0.5x_{j3} + 2x_{j1}x_{j3}),$$

$$\tilde{\theta}_{2j} = \Phi_{0,1.5}(-x_{j1} - 2x_{j3}),$$

$$\tilde{\theta}_{3j} = \Phi_{0,1.5}(x_{j1} - 1.5x_{j2} - 2x_{j1}x_{j2}).$$

See Figure 2 for response surfaces versus biomarkers 1 and 2 given the third biomarker values of $x_3 = 0.6$ and $x_3 = -0.6$. In this scenario, each of the three treatments can yield the highest response rate in some area of the biomarker space and the ordering of treatment effects is related to all three biomarkers in a nonlinear and complex fashion.

In scenario 3, $T = 2$ treatments are considered and $B = 2$ biomarkers are related to the response rate. We assume that the true response rates are

$$\tilde{\theta}_{1,j} = \Phi_{0,1.5}(x_{j1}^2/2 + x_{j1}x_{j2}/2),\ \ \tilde{\theta}_{2,j} = \Phi_{0,1.5}(x_{j2}^2/2 - x_{j1}x_{j2}/2).$$

Figure 2 displays the response rate surfaces versus biomarkers 1 and 2 under each treatment. Different from scenarios 1 and 2, the response surfaces are non-monotone due to the second-order terms in the formula. Also, the differences in the effect sizes between the two treatments are small across the biomarker space, making it challenging to detect the winning treatment and subgroups.

In scenario 4, we assume a saddle-shape curve for the true response rates, given by

$$\tilde{\theta}_{1j} = \Phi(x_{j1}^2 - x_{j2}^2),\ \ \tilde{\theta}_{2j} = \Phi(x_{j2}^2 - x_{j1}^2).$$

The response surfaces are also plotted in Figure 2.

In scenarios 5 and 6, we consider linear boundaries for $T = 2$ treatments and $B = 2$ biomarkers. The bottom row of Figure 2 shows the true partition and the response rate for each true partition set. In scenario 5, both biomarkers are predictive and partition boundaries depend on both biomarker values. In scenario 6, two biomarkers are predictive of response under treatment 1, and only biomarker 2 is predictive of response rates under treatment 2. Also, the boundaries in scenario 6 are parallel to the biomarker axes.

4.2. Simulation Results

4.2.1. Subgroup-Treatment Pair (STPs)—We first report STPs after a trial is complete. The estimated STPs are either based on a grid of 101 × 101 evenly spaced points for the two-dimensional biomarker space, or on a grid of 101 × 101 × 101 evenly spaced points for the three-dimensional biomarker space, according to the method in Section 3.2. We arbitrarily select one trial for each scenario as an example. The estimated STPs for the selected trials in scenarios 1 and 3–6 are plotted in Figure 3 along with their simulation truth of the partition. From the left to right column, results for scenarios 1, and 3–6 are plotted sequentially. And the estimated STPs for one trial in scenario 2 are shown in Figure 4. As scenario 2 involves three biomarkers and hence a graphical display of STPs is challenging, we plot two planes in the two-dimensional space of (x_1, x_2) for fixed values of $x_3 = 0.6$ and $x_3 = -0.6$. In Figure 3, the top panels of scenarios 3–6 show the simulation truth of the partition on the biomarker space by heatmap of differences in the true response rates between two treatments, and the top panel of scenario 1 shows the heatmap of response rate difference between treatments 1 and 3. In Figure 4, the top panels show the wining treatment by color (light gray-treatment 1, dark gray-treatment 2 (or treatment 3 in scenario 1)). The bottom panels of both Figures 3 and 4, report the estimated STPs with $(1 - \alpha)$ confidence levels by color, where regions with deep color and light color correspond to the estimated STPs under $\alpha = 0.1$ and $\alpha = 0.2$, respectively. Comparing the subgroup truth in top panels and the estimated STPs in bottom panels, we can see that the estimated STPs are subsets of the true subgroups largely, especially for scenarios 1–4. Because scenario 3 is a hard case as

stated in Section 4.1, SCUBA does not find any STPs in the selected trial based on $N = 400$ patients and $\alpha = 0.1$ or 0.2.

Defining the STP false discovery rate (STP-FDR) as the fraction of the grid points that report the wrong winning treatment or are outside the true subgroups among declared STPs, we report the mean and standard deviation of STP-FDRs over 1000 trials for each scenario in Table 1. We list results for both $\alpha = 0.1$ and $\alpha = 0.2$. The results show that the STP-FDR of SCUBA is well controlled, for both $\alpha = 0.1$ and $\alpha = 0.2$. More importantly, the standard deviations are all small, suggesting there is limited trial-to-trial variability.

The SUBA and BART methods do not provide STP estimates.

4.2.2. Patient Allocation—Next, we compare the patient allocation under SCUBA, SUBA, and BART. A common goal of all three designs is to enrich patients allocation to the superior treatment with a higher response rate based on the biomarker information. According to the simulation truth, we find S_t, a subset in Ω, as the true subgroup in the biomarker space in which patients have a higher response rate under treatment t than all the other treatments. In other words, S_t is the true optimal subgroup for treatment t. If a patient in S_t is assigned to treatment t by a given design, the design does the right thing. Otherwise, the design makes a mistake.

To evaluate the performance of patient allocation, we then compute the average number of patients (ANP) assigned to each treatment in each subgroup after the run-in phase. Let $NP_{t,\tilde{t}}^{(w)} = \sum_{j=n+1}^{N} \mathbf{1}(t_j^w = \tilde{t}, \boldsymbol{x}_j^w \in S_t)$ be the number of patients allocated to treatment t^ who belong to the true subgroup S_t after run-in phase in the w^{th} simulated trial, where tjw and $\boldsymbol{x}jw$ are the treatment assignment and biomarker profile, respectively, for patient j in the w^{th} simulated trial. Then

$$ANP_{t,\tilde{t}} = \sum_{w=1}^{1000} NP_{t,\tilde{t}}^{(w)}/1000.$$

The results of ANP for all scenarios are listed in Table 2.

In scenario 0, where the response rates for all the patients under either treatment are 0.4, all three designs do not favor either of the two treatments and assigns patients equally to the two treatments. In scenario 1, the response rate is monotonic with respect to either of the biomarkers when the other biomarker is fixed. Here, $S_1 = \{j : x_{j,2} > 0\}$ and $S_3 = \{j : x_{j,2} < 0\}$, and treatment 2 can never be the superior arm over the other two treatments. It can be seen that SUBA does slightly better than SCUBA in scenario 1 as it assigns more patients to the superior treatment. The reason is that the truth agrees with SUBA's assumption. In other words, the underlying partition model for scenario 1, that is, dividing the population using the line $x_2 = 0$, happens to be the median of x_2, which is used by SUBA as subgroup boundaries.

In scenarios 2–6, SCUBA outperforms SUBA consistently with more patients allocated to the correct superior arms. The results demonstrate the desirability of SCUBA in adaptively learning the subgroup pattern throughout the trials. In these scenarios, the dose-response curves are more complex, making SCUBA a more desirable design.

BART performs slightly better than SCUBA in scenarios 1 and 4, while SCUBA outperforms BART slightly in scenarios 3 and 6. However, BART dose not perform well in either scenario 2, with more than half of the patients in S_2 allocated to treatments 1 and 3, or scenario 5, with most patients in S_2 allocated to treatment 1.

5. Discussion

We propose a novel design for multi-arm clinical trials. SCUBA can identify the subgroups of patients having different response rates to specific treatments. This is in the essence of precision medicine. SCUBA allocates patients adaptively based on observed data during the trial and reports STPs at the end of the trial for future confirmatory studies with low false discovery rates. Our method is fully Bayesian, providing principled and coherent inference on the partition and STPs. Compared to BART and SUBA, SCUBA is more flexible and capable of capturing irregular subgroups with complex boundaries, as shown in the simulation study.

We consider binary outcomes and continuous biomarkers in SCUBA, although the proposed method can be easily extended to continuous outcomes and discrete biomarker variables. For continuous or survival outcomes, we only need to change the sampling model $L(\boldsymbol{y} \mid \boldsymbol{\theta}, \prod)$ and modify the base distribution for the DP prior. For discrete covariates, the random partition model becomes easier since discrete covariates have natural boundaries that do not need modeling.

The rule for STP reporting is flexible, and we could tune the confidence level α in inequality (6) depending on the objective of studies. Besides, by simple modification to equation (6) one can allow two treatments to be selected if both of them exhibit higher response rates than a standard therapy.

SCUBA allows disjoint subgroups in the biomarker space to be allocated to the same STP. In reality, this might be unlikely, unless the biomarkers are related to the drug in an antagonistic fashion. That is, the drug works well when only one of the biomarker is upregulated, but not both. It could also be possible when more than two biomarkers are predictive, forming potential complex subgroups. These subgroups could be approximated using hypercubes for practical reasons, such as ease of interpretation.

We consider equally spaced grid in reporting STPs because averaging over all random partitions is challenging. Instead, we infer the winning treatment at each grid point based on the posterior sample of random partitions. One could use an “adaptive” grid where the grid size is sparse or dense when few or many data points are available. This could reduce the overall computation by a small factor. Lastly, in the inference of STPs one could also select STPs based on a utility function that takes into account features of the subgroups, such as subgroup size, so that smaller subgroups can be filtered.

The main limitation of SCUBA is that the time to observe patient outcome needs to be relatively short, since SCUBA uses adaptive enrichment scheme after run-in phase. In the case of having a long-term outcome, we could modify the current method to accommodate missing response values, which will be a future topic.

Supplementary Material

Refer to Web version on PubMed Central for supplementary material.

Acknowledgments

Yuan Ji's research is partly supported by NIH R01 132897-06 and Dan Catenacci's research is partly supported by NIH K23 CA178203. We thank the Associate Editor and two anonymous reviewers for their constructive comments which improved the quality of the article.

References

Ala U, Karreth FA, Bosia C, Pagnani A, Taulli R, Léopold V. Integrated transcriptional and competitive endogenous rna networks are cross-regulated in permissive molecular environments. Proceedings of the National Academy of Sciences. 2013; 110:7154–7159.

Berger JO, Wang X, Shen L. A bayesian approach to subgroup identification. Journal of Biopharmaceutical Statistics. 2014; 24:110–129. [PubMed: 24392981]

Catenacci DV. Next-generation clinical trials: Novel strategies to address the challenge of tumor molecular heterogeneity. Molecular Oncology. 2015; 9:967–996. [PubMed: 25557400]

Chipman HA, George EI, McCulloch RE. Bart: Bayesian additive regression trees. The Annals of Applied Statistics. 2010; 4:266–298.

Ferguson TS. A bayesian analysis of some nonparametric problems. The Annals of Statistics. 1973; 1:209–230.

Foster JC, Taylor JM, Ruberg SJ. Subgroup identification from randomized clinical trial data. Statistics in Medicine. 2011; 30:2867–2880. [PubMed: 21815180]

Freidlin B, McShane LM, Korn EL. Randomized clinical trials with biomarkers: Design issues. Journal of the National Cancer Institute. 2010

Green DP, Kern HL. Modeling heterogeneous treatment effects in survey experiments with bayesian additive regression trees. Public Opinion Quarterly. 2012; 76:491–511.

Green PJ. Reversible jump markov chain monte carlo computation and bayesian model determination. Biometrika. 1995; 82:711–732.

Hjort, NL., Holmes, C., Müller, P., Walker, SG. Bayesian Nonparametrics. Vol. 28. New York: Cambridge University Press; 2010.

Kim ES, Herbst RS, Wistuba II, Lee JJ, Blumenschein GR, Tsao A. The battle trial: Personalizing therapy for lung cancer. Cancer Discovery. 2011; 1:44–53. [PubMed: 22586319]

Laud, PW., Sivaganesan, S., Müller, P. Bayesian theory and applications. Oxford: Oxford University Press; 2013. p. 576-592.chapter Subgroup Analysis

Lipkovich I, Dmitrienko A, Denne J, Enas G. Subgroup identification based on differential effect search–A recursive partitioning method for establishing response to treatment in patient subpopulations. Statistics in Medicine. 2011; 30:2601–2621. [PubMed: 21786278]

Maitournam A, Simon R. On the efficiency of targeted clinical trials. Statistics in Medicine. 2005; 24:329–339. [PubMed: 15551403]

McLachlan, G., Peel, D. Finite mixture models. New York: John Wiley & Sons; 2004.

Mullard A. Nci-match trial pushes cancer umbrella trial paradigm. Nature Reviews Drug Discovery. 2015; 14:513–515.

Neal RM. Markov chain sampling methods for dirichlet process mixture models. Journal of Computational and Graphical Statistics. 2000; 9:249–265.

Richardson S, Green PJ. On bayesian analysis of mixtures with an unknown number of components (with discussion). Journal of the Royal Statistical Society, Series B (Statistical Methodology). 1997; 59:731–792.

Ruberg SJ, Chen L, Wang Y. The mean does not mean as much anymore: Finding sub-groups for tailored therapeutics. Clinical Trials. 2010

Sargent DJ, Conley BA, Allegra C, Collette L. Clinical trial designs for predictive marker validation in cancer treatment trials. Journal of Clinical Oncology. 2005; 23:2020–2027. [PubMed: 15774793]

Shen J, He X. Inference for subgroup analysis with a structured logistic-normal mixture model. Journal of the American Statistical Association. 2015; 110:303–312.

Simon R, Maitournam A. Evaluating the efficiency of targeted designs for randomized clinical trials. Clinical Cancer Research. 2004; 10:6759–6763. [PubMed: 15501951]

Sivaganesan S, Laud PW, Müller P. A bayesian subgroup analysis with a zero-enriched polya urn scheme. Statistics in Medicine. 2011; 30:312–323. [PubMed: 21225894]

Xu Y, Trippa L, Müller P, Ji Y. Subgroup-based adaptive (suba) designs for multi-arm biomarker trials. Statistics in Biosciences. 2014; 8:1–22. [PubMed: 27594925]

Zhao L, Tian L, Cai T, Claggett B, Wei LJ. Effectively selecting a target population for a future comparative study. Journal of the American Statistical Association. 2013; 108:527–539. [PubMed: 24058223]

Box 1

The SCUBA design

1. **Run-in.** Start the trial. The first $n \leq N$ patients are randomized equally to T treatments.
2. **Adaptive allocation.** For the $(n+1)^{th}$ patient, calculate posterior predictive probability $q_{n+1}(t)$, and allocate treatment $\hat{t} = \arg\max_t q_{n+1}(t)$ to the patient or randomize to treatment t with the probability proportional to $q_{n+1}(t)$.
3. **Posterior updating.** Repeat step 2 for patients $n+2, \cdots, N$.
4. **Report on subgroups.** Upon conclusion of the trial, make a recommendation of STPs based on desired confidence α.

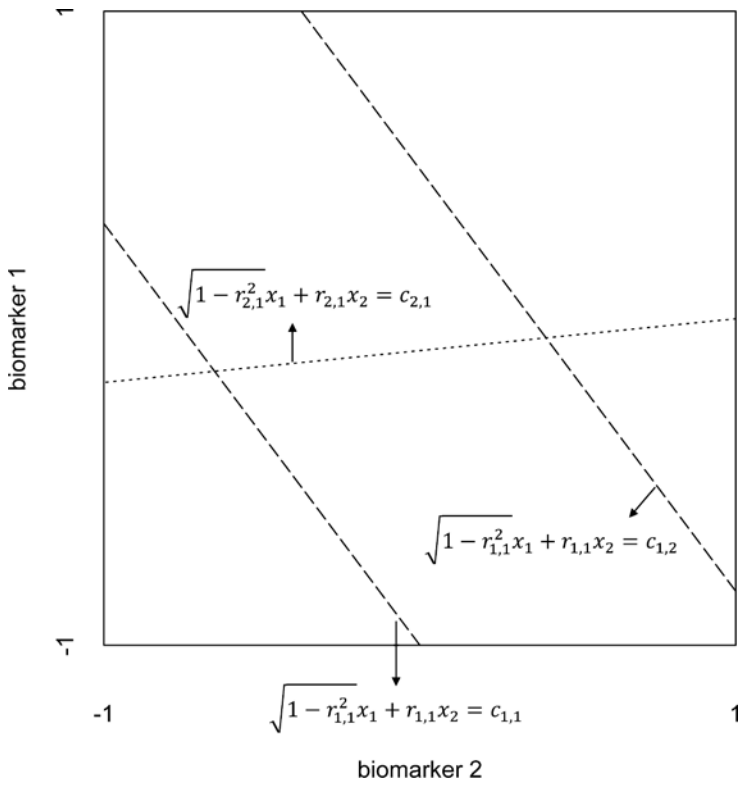

Figure 1.

An example of partition of a 2-d biomarker space. There are $\boldsymbol{B} = 2$ directions, with $\boldsymbol{M}_1 = 2$ and $\boldsymbol{M}_2 = 1$ linear boundaries for each direction, respectively.

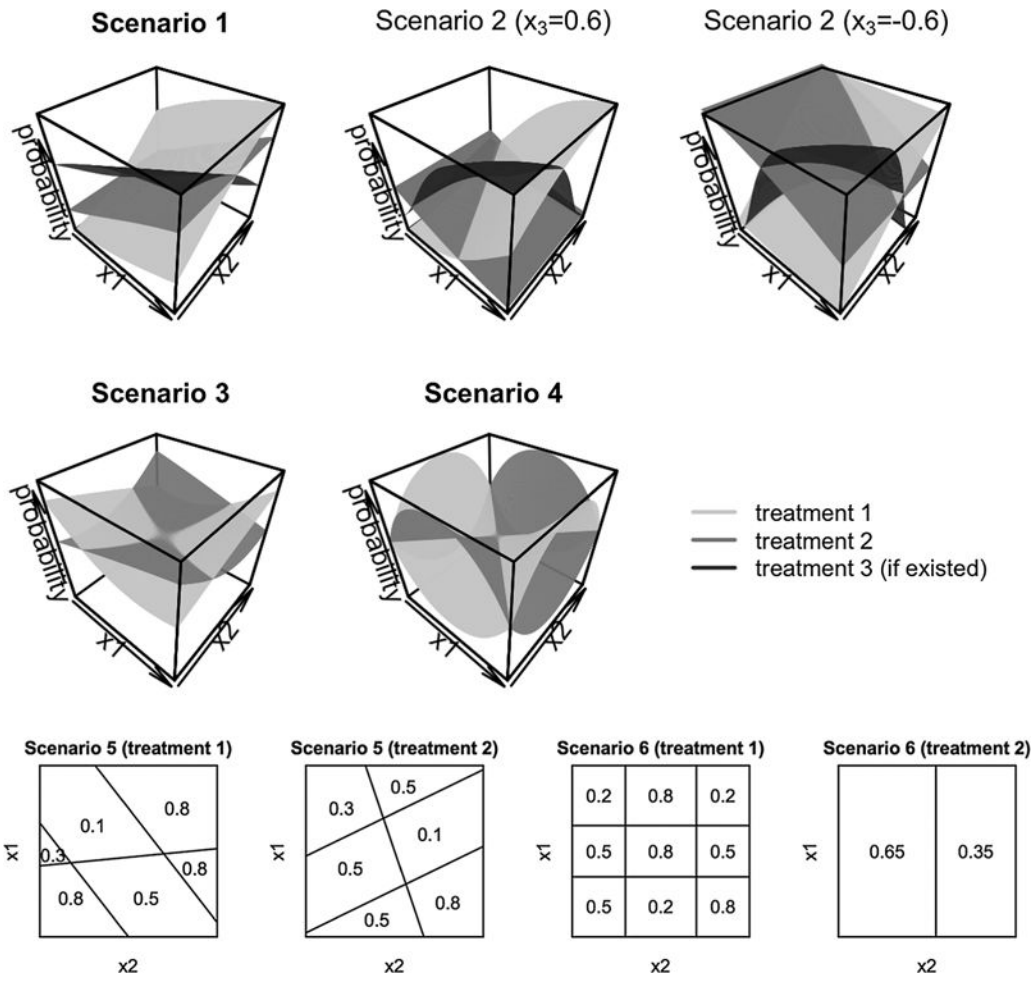

Figure 2. Top and middle rows

True response surfaces for scenarios 1–4 in the simulation (light gray-treatment 1, medium gray-treatment 2, dark gray-treatment 3 (if existed)). **Bottom row:** True partitions and response rates in each partition set for scenarios 5 and 6 in the simulation.

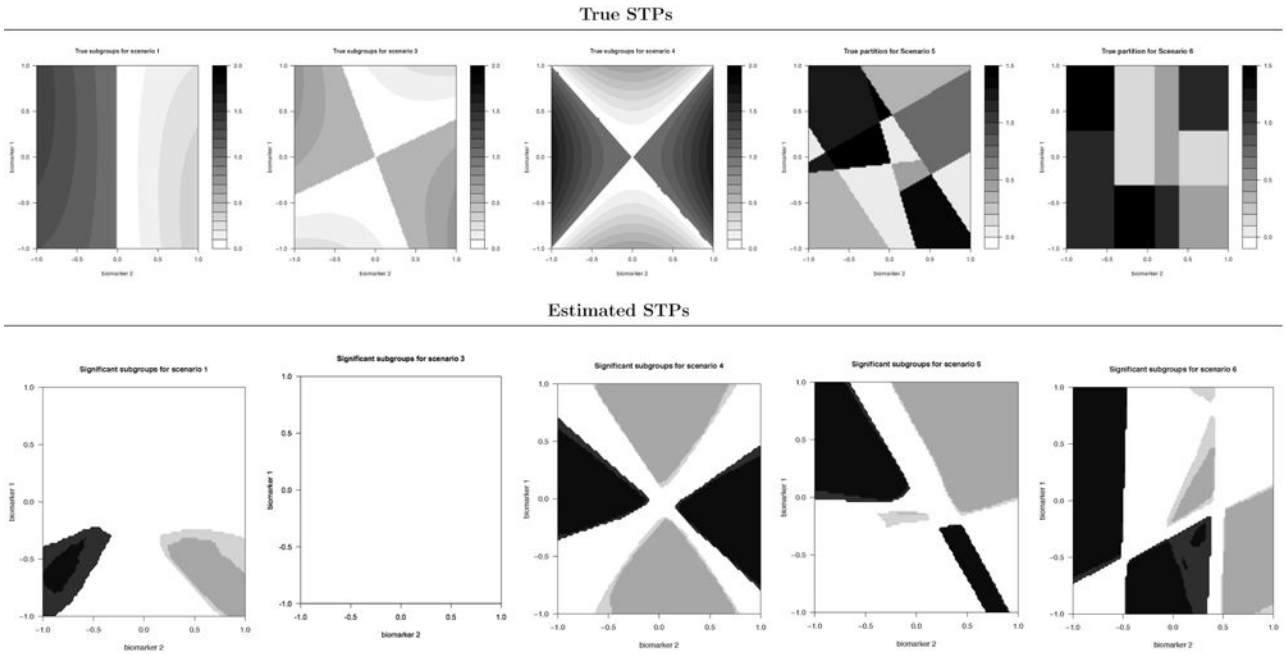

Figure 3.

True partitions and STPs for scenarios 1, and 3–6. The first row shows the true STPs with light gray/dark gray color representing the true winning treatment (light gray-treatment 1, dark gray-treatment 2 (or treatment 3 in scenario 1)), respectively. The second row plots the estimated STPs (light gray-treatment 1, dark gray-treatment 2 (or treatment 3 in scenario 1)) based on the marginal inference $Pr(\theta_i > \theta_j \mid data) > 1 - \alpha$ in Section 3.2, with $\alpha = 0.1$ for deep color and $\alpha = 0.2$ for light color. From the left column to the right, the plots gives the true partition and reported STPs based on a simulated trial for scenario 1, and 3–6, respectively.

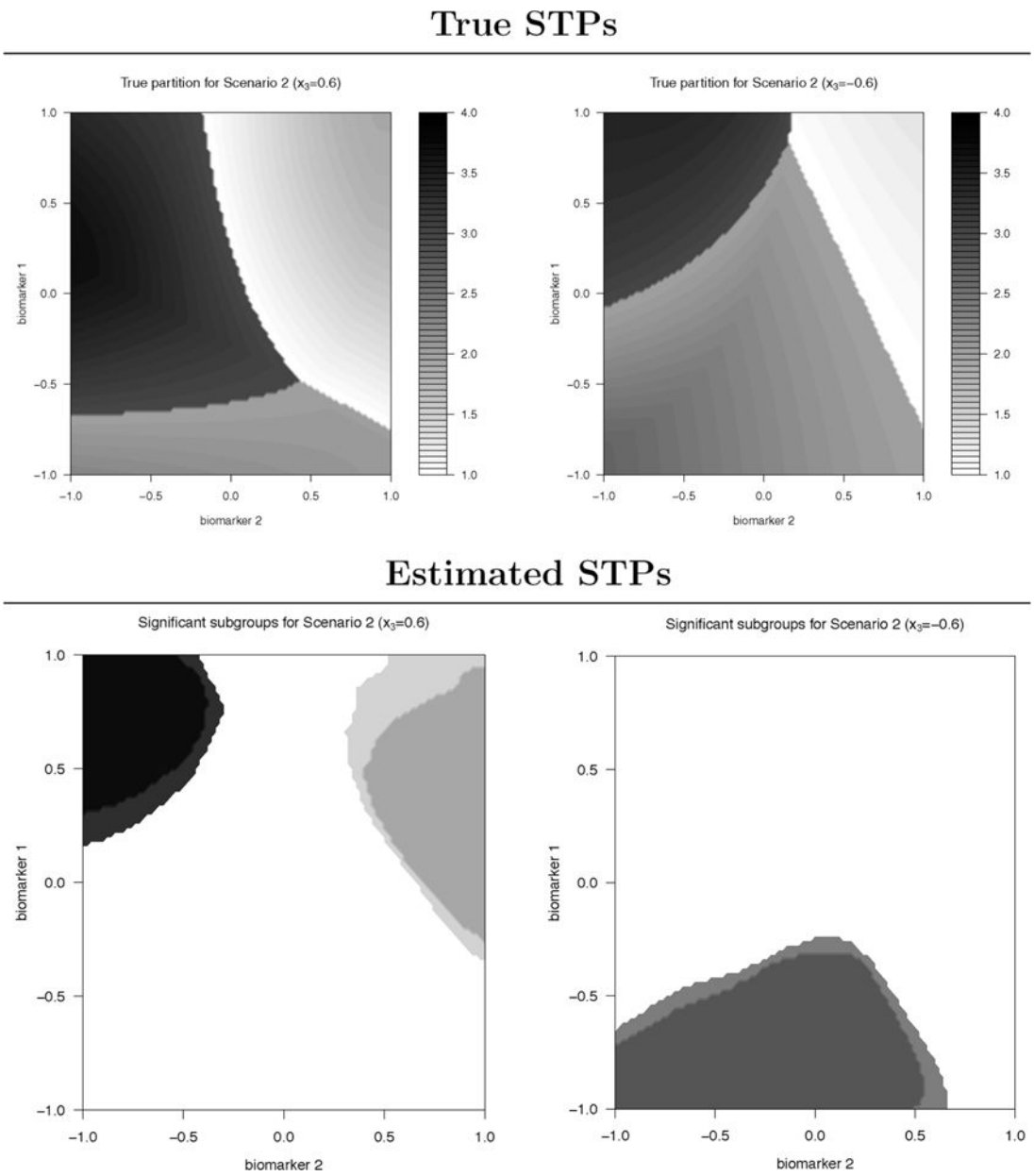

Figure 4.

True partitions and STPs for scenarios 2. The left and right columns show the results for the dose-response plane when $x_3 = 0.6$ and $x_3 = -0.6$, respectively. Light gray, medium gray, and dark gray colors denote the target subgroups for treatments 1, 2, and 3, respectively. The gradient colors in the top row indicate differences in the response rates between the top two treatments.

Table 1

Mean (standard deviation) of STP-FDRs across 1000 trials of each scenario, for $\alpha = 0.1$ and $\alpha = 0.2$

Scenario	$\alpha = 0.1$	$\alpha = 0.2$
1	0.009 (0.074)	0.017 (0.076)
2	0.022 (0.033)	0.038 (0.040)
3	0.082 (0.183)	0.115 (0.194)
4	0.034 (0.062)	0.051 (0.070)
5	0.063 (0.060)	0.094 (0.063)
6	0.050 (0.079)	0.066 (0.080)

Table 2

The average number of patients assigned to each treatment after the run-in phase among different subsets of patients. Here, S_t denotes the true subgroup for treatment t, in which patients have higher response rates under treatment t than all the other treatments according to the simulation truth. Bold (normal)-font numbers are correct (wrong) allocations regarding the simulation truth.

		SCUBA			SUBA			BART		
Scenario	**Subset**	**1**	**2**	**3**	**1**	**2**	**3**	**1**	**2**	**3**
0	\	49.51	50.49	\	48.90	51.10	\	49.34	50.66	\
1	S_1	**38.66**	8.09	3.33	**41.49**	6.39	2.21	**43.81**	4.24	2.03
	S_3	3.40	8.27	**38.25**	2.49	6.60	**40.83**	2.28	4.32	**43.33**
2	S_1	**22.42**	3.95	2.56	**20.88**	5.13	2.92	**25.02**	1.65	2.56
	S_2	5.14	**29.04**	3.92	6.79	**25.37**	5.94	11.54	**18.33**	8.22
	S_3	3.65	4.18	**25.14**	2.63	5.80	**24.53**	3.73	3.20	**26.04**
3	S_1	**29.40**	20.65	\	**27.71**	22.35	\	**27.76**	22.30	\
	S_2	21.06	**28.89**	\	24.50	**25.44**	\	22.18	**27.77**	\
4	S_1	**35.21**	14.70	\	**34.40**	15.50	\	**39.70**	10.20	\
	S_2	12.52	**37.57**	\	15.37	**34.73**	\	10.37	**39.73**	\
5	S_1	**50.84**	14.02	\	**49.48**	15.38	\	**50.42**	14.45	\
	S_2	5.44	**29.69**	\	7.23	**27.91**	\	26.50	**8.63**	\
6	S_1	**35.09**	10.53	\	**33.46**	12.16	\	**32.55**	13.07	\
	S_2	12.09	**42.30**	\	13.66	**40.72**	\	17.62	**36.76**	\